High-coherence ultra-broadband bidirectional dual-comb fiber laser

doi: 10.1364/OE.27.005931

Research Article | Vol. 27, No. 5 | 4 Mar 2019 | OPTICS EXPRESS 5931
Optics EXPRESS

High-coherence ultra-broadband bidirectional dual-comb fiber laser

YOSHIAKI NAKAJIMA,[1,2] YUYA HATA,[1,2] AND KAORU MINOSHIMA[1,2,*]

[1]*Department of Engineering Science, Graduate School of Informatics and Engineering, University of Electro-Communications, 1-5-1 Chofugaoka, Chofu, Tokyo 182-8585, Japan*
[2]*Japan Science and Technology Agency (JST), ERATO, MINOSHIMA Intelligent Optical Synthesizer (IOS) Project, 1-5-1 Chofugaoka, Chofu, Tokyo 182-8585, Japan*
k.minoshima@uec.ac.jp

Abstract: Dual-comb spectroscopy has emerged as an attractive spectroscopic tool for high-speed, high-resolution, and high-sensitivity broadband spectroscopy. It exhibits certain advantages when compared to the conventional Fourier-transform spectroscopy. However, the high cost of the conventional system, which is based on two mode-locked lasers and a complex servo system with a common single-frequency laser, limits the applicability of the dual-comb spectroscopy system. In this study, we overcame this problem with a bidirectional dual-comb fiber laser that generates two high-coherence ultra-broadband frequency combs with slightly different repetition rates (f_{rep}). The two direct outputs from the single-laser cavity displayed broad spectra of > 50 nm; moreover, an excessively small difference in the repetition rate (< 1.5 Hz) was achieved with high relative stability, owing to passive common-mode noise cancellation. With this slight difference in the repetition rate, the applicable optical spectral bandwidth in dual-comb spectroscopy could attain ~479 THz (~3,888 nm). In addition, we successfully generated high-coherence ultra-broadband frequency combs via nonlinear spectral broadening and detected high signal-to-noise-ratio carrier–envelope offset frequency (f_{CEO}) beat signals using the self-referencing technique. We also demonstrated the high relative stability between the two f_{CEO} beat signals and tunability. To our knowledge, this is the first demonstration of f_{CEO} detection and frequency measurement using a self-referencing technique for a dual-comb fiber laser. The developed high-coherence ultra-broadband dual-comb fiber laser with capability of f_{CEO} detection is likely to be a highly effective tool in practical, high-sensitivity, ultra-broadband applications.

1. Introduction

Optical frequency combs have emerged as indispensable tools in various scientific and technical fields [1,2]. In the late 1990s, carrier–envelope offset frequency (f_{CEO}) detection and stabilization were achieved using a self-referencing technique [3–5]. Subsequently, full phase stabilization of the repetition rate (f_{rep}) and f_{CEO} was also achieved. Optical frequency combs are used in several applications such as frequency metrology [6–9], high-precision spectroscopy [10], high-precision microwave generation [11,12], optical communications [13], arbitrary waveform generation [14], astronomical spectrograph calibration [15,16], and absolute distance measurements [17].

In spectroscopy using frequency combs, the amplitude and phase of the individual comb modes store the information of samples, i.e., atom and molecular absorption and phase spectra, in the optical frequency domain. Therefore, mode-resolved spectroscopy could realize ultra-high precision spectroscopy, in which the spectral resolution is ultimately limited by the comb mode linewidth. Toward this objective, several methods have been proposed and demonstrated, e.g., the combination of an optical grating and a Fabry–Perot cavity [18,19], a virtually imaged phased array (VIPA) [10], and Fourier transform spectroscopy (FTS) [20,21].

In particular, dual-comb spectroscopy (DCS) techniques [22,23] have various advantages when compared to previous techniques in term of the rapid acquisition of each interferogram, the sensitivity, and the resolution. The sensitivity can be improved by coherent averaging. The spectral point spacing is primary set by the comb f_{rep}, and it can

#347230 https://doi.org/10.1364/OE.27.005931
Journal © 2019 Received 1 Oct 2018; accepted 7 Feb 2019; published 20 Feb 2019

Optics EXPRESS

be further improved by f_{rep} scanning or the discrete Fourier transform technique [24] at the expense of the measurement speed. The frequency precision is limited by the underlying frequency comb reference. The DCS is FTS techniques wherein multi-heterodyne detection is performed using two optical frequency combs with slightly different f_{rep}. In these techniques, by placing the sample in one of the comb (signal comb) optical path, the absorption and phase information of the sample are stored in each comb mode of the signal comb; moreover, the information could be retrieved precisely from the interferogram between the signal comb and the other comb (local comb). Specifically, the two frequency combs with slightly different f_{rep}s sample each other without a mechanical moving stage owing to the scanning of their relative time delay between two pulse trains in the time domain. In the frequency domain, the interferogram can be considered as multi-heterodyne beat detection of the two frequency-comb modes; here, the optical frequency combs are down-converted into a single radio-frequency (RF) comb. The information in the optical domain can be retrieved from the amplitude and phase of the individual comb modes [25]. As a scan-less interferometry, DCS provides advantages over the conventional FTS with regard to measurement speed and resolution.

Because of its remarkable capabilities, DCS has been adopted in several applications, e.g., broadband, high-precision, high-resolution gas spectroscopy [26,27], high-speed solid-state spectroscopy [28,29], time-resolved spectroscopy [30], nonlinear spectroscopy [31,32], terahertz spectroscopy [33], optical sensing [34,35], distance measurement [36], microscopy [37], and imaging [38]. These applications require high sensitivity. If the two frequency combs are not mutually coherent or relatively stable, the averaging of interferogram is distorted. Meanwhile, the coherent averaging of the interferogram can improve the measurement sensitivity. Thus, there is a demand for the two frequency combs to exhibit high relative coherence and stability.

The previous dual-comb system employs two independent mode-locked lasers for generating two optical frequency combs with slightly different f_{rep}s. As these lasers exhibit independent fluctuations in their f_{rep} and f_{CEO} in the free-running state, the interferogram is distorted. Therefore, a servo system and signal processing are typically used for high relative coherence between the two frequency combs. Various schemes have been proposed to fulfill the requirement, e.g., relative stabilization with a single reference continuous-wave (cw) laser [25–27], real-time compensation of relative phase fluctuation [39], and adaptive sampling [40]. In addition, a fieldable DCS system [35,41] based on two polarization-maintaining fiber lasers [42] has been demonstrated; it could broaden the applicability of the DCS. Notwithstanding the capabilities of DCS in a broad research area, the use of the dual-comb technique is still mainly limited to researchers with expertise owing to the high cost of similar systems based on two lasers and the servo systems. Therefore, a simple and turnkey dual-comb source could offer an attractive alternative solution for a broad range of users.

In recent years, the dual-comb laser, which emits two optical frequency combs from a single-laser cavity with a small difference in their f_{rep} values, has attracted considerable attention owing to its advantageous properties such as passive mutual coherence and common-mode noise cancellation. Numerous schemes have been reported such as a dual-comb laser with an Er-doped ZBLAN chip [43], a Kerr-lens mode-locked bidirectional Ti:sapphire laser [44], and a mode-locked integrated external-cavity surface emitting laser (MIXSEL) [45]. In addition, a micro-resonator based dual-comb source on the same chip from a single pump laser has been reported [46]. Although these lasers exhibit remarkable capabilities such as broadband spectrum, ultra-short pulse, integration, and high repetition rate, a dual-comb laser with high practicability and robustness is essential for extending the application of the DCS technique beyond research laboratories. Meanwhile, a frequency comb based on a mode-locked fiber laser has been widely used as a standard system since it was first reported in the early 2000s [47,48]. Fiber-based frequency combs are inexpensive, compact, and robust owing to their all-fiber-based configuration [49]; moreover, they can generate low phase noise frequency combs [50]. Therefore, numerous DCS systems have been demonstrated with two mode-locked fiber lasers because of their practical features. Recently, dual-wavelength [51] and

Optics EXPRESS

bidirectional [52] mode-locked Er-fiber lasers have been demonstrated as dual-comb fiber lasers for real-time gas spectroscopy and terahertz spectroscopy. However, the demonstrated spectral bandwidth of the dual-comb fiber laser was of the order of a few nanometers with the anomalous cavity dispersion; this is considerably narrower than that of a typical low-noise Er-fiber-based frequency comb operating at the near zero cavity dispersion regime [50]. This narrow output spectrum and cavity dispersion indicates the presence of large phase noise. However, as it is important for the seed frequency comb to exhibit high coherence for nonlinear spectral broadening, it is challenging to expand the spectral bandwidth with high coherence. In [53], a supercontinuum was generated using a highly nonlinear fiber (HNLF). However, the detection of f_{CEO} beat notes using a dual-comb fiber laser has not been reported until the present. Moreover, in [51,52], a saturable absorber was shared between two frequency combs in the laser cavity; thus, undesirable nonlinear interactions between two pulses at the saturable absorber could cause instability [43]. In particular, such a strong nonlinear interaction at the saturable absorber could induce self-synchronization between the two pulses [54]; thus, it would not be feasible to achieve an excessively marginal difference in the repetition rate (Δf_{rep}). Realizing a small Δf_{rep} is essential for broad bandwidth detection in DCS. Finally, in addition to the limitation in the design of the physical configuration of the cavity, it is challenging to optimize both the outputs simultaneously. This limits the degrees of freedom for tuning Δf_{rep}.

In this study, to overcome the problems arising from low-coherence supercontinuum generation and the limitation in generating marginal Δf_{rep}, we proposed and developed a bidirectional mode-locked Er-fiber laser using novel concepts in the laser cavity configuration, i.e., the symmetrical cavity configuration and a combination of two mode-locking mechanisms. We used a combination of two saturable absorber mirrors (SAMs) and nonlinear polarization rotation (NPR) as a mode-locking mechanism; this facilitated the generation of low phase noise frequency combs. The two direct outputs from the laser cavity displayed broad spectra with a full-width-at-half-maximum (FWHM) bandwidth of ~56 nm. Moreover, we successfully generated high-coherence ultra-broadband frequency combs by nonlinear spectral broadening and detected the high signal-to-noise-ratio (SNR) f_{CEO} beat signals in both the directions. A high relative stability between the two f_{CEO} beat signals was also demonstrated without active stabilization. To our knowledge, this is the first demonstration of f_{CEO} detection and frequency measurement using a self-referencing technique for a dual-comb fiber laser. Because f_{CEO} is one of the only two parameters of frequency combs, it is required for absolute frequency measurement in high-accuracy spectroscopy. In the case of DCS, detecting and regulating the f_{CEO} is important for high-precision spectroscopy as well as for high-sensitivity using coherent averaging. In addition, the controllability of f_{CEO} is also important for various applications utilizing coherence, such as coherent spectroscopy, nonlinear spectroscopy, and phase imaging. Moreover, such a high-coherence ultra-broadband supercontinuum can be further converted to other wavelength regions with high coherence for a wide range of applications. Furthermore, to suppress high nonlinearity in a saturable absorber, we use two SAMs in the laser cavity that are not shared between the two pulses, on the basis of a configuration similar to that described in [55]. As a result, an excessively small Δf_{rep} (< 1.5 Hz; f_{rep} = 38 MHz) was achieved with high stability. As these two frequency combs were generated by the same single-laser cavity, a high relative stability between the two frequency combs could be realized via passive common-mode noise cancellation. With this small Δf_{rep}, the applicable optical spectral bandwidth in DCS can reach ~479 THz (~3,888 nm). Finally, the developed high-coherence ultra-broadband dual-comb fiber laser is likely to be a highly effective tool in practical ultra-broadband spectroscopy in a broad application area.

2. Experimental setup and results

2.1 Setup of bidirectional dual-comb fiber laser

Figure 1 shows a schematic of the developed bidirectional dual-comb fiber laser with the symmetrical cavity configuration and a combination of two mode-locking mechanisms. It

Optics EXPRESS

consists of a single-mode fiber (SMF) and an Er-doped fiber (EDF), which is bidirectionally pumped by a 976-nm laser diode (LD) via two wavelength division multiplexing (WDM) couplers. The two 10/90 couplers are placed symmetrically in the laser cavity with respect to the EDF, and 10% of the propagating power is coupled out of the cavity via a coupler. Conventionally, a unidirectional ring cavity with an in-line isolator facilitates self-starting of passive mode locking. For a bidirectional mode-locked fiber laser, an in-line isolator is not included in the laser cavity; moreover, it can be operated in both the clockwise (CW) and counter-clockwise (CCW) directions. The counter-propagating pulses are separated via two 50/50 couplers and two three-port circulators; furthermore, they are launched into two separate SAMs to suppress undesirable highly nonlinear interaction between two co-propagating pulses at a saturable absorber. All the components are installed in the cavity symmetrically to optimize the mode-locking operation in both the directions simultaneously. Moreover, all the non-common paths are placed close together for common-mode noise cancellation. In the developed cavity configuration, Δf_{rep} can be conveniently tailored by the path length in the separated region consisting of the SMF and free-space. Furthermore, we installed an in-line polarization controller comprising a half-wave plate (H), a quarter-wave plate (Q), and a polarizer (P) in the cavity to ensure mode locking based on the NPR mechanism. Such a combination of slow and fast mode-locking mechanisms is likely to generate low phase noise frequency combs and stabilize the mode-locking operation in both the directions simultaneously [56,57]. The net dispersion of the laser cavity was estimated to be - 0.06 ps^2 at 1,550 nm. In a future work, all the free-space setups can be integrated to further reduce the size using micro-optic packaging; moreover, the two 50/50 couplers and circulators can be modified into a four-port circulator. In this study, all the experiments were conducted in free-running operation as described in later sections.

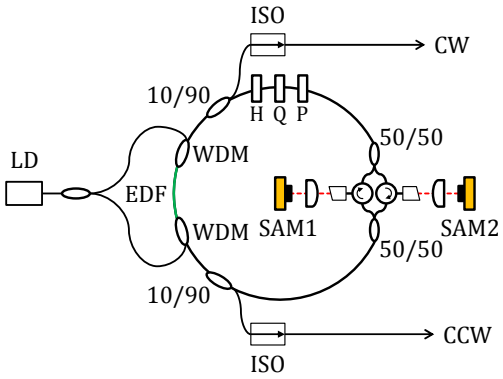

Fig. 1. Experimental setup of bidirectional dual-comb fiber laser with nonlinear polarization rotation (NPR) and saturable absorber mirrors (SAMs). LD: laser diode; EDF: Er-doped fiber; WDM: wavelength division multiplexing coupler; H and Q: half- and quarter-wave plate; P: polarizer; 10/90 and 50/50: 10/90 and 50/50 coupler; ISO: isolator; CW and CCW: clockwise and counter-clockwise outputs.

2.2 Characteristics of the two outputs of dual-comb fiber laser

As shown in Fig. 2(a), the two outputs from the laser cavity simultaneously and directly displayed broad spectra with a FWHM bandwidth of ~56 nm at ~1,550 nm. These bandwidths are the broadest reported till date in the case of the dual-comb fiber laser. In addition, both the unidirectional mode-locking outputs exhibited almost identical broad spectra. Thus, such broad spectra were not caused by nonlinear interaction between the two counter-propagating pulse trains. Furthermore, the average powers of the two outputs were adequately balanced (1.8 mW (CW) and 1.2 mW (CCW)) with the total pump power of approximately 650 mW at 976 nm. This was achieved because the mode-locking operation could be optimized in both the directions simultaneously; this in turn was because the two SAMs were not shared in the two frequency combs, both NPR and

Optics EXPRESS

SAM were used, and the cavity configuration was symmetrical. Such a broad bandwidth of the fiber-based frequency comb from the direct laser output indicated the presence of low phase noise [49,50,58,59]; furthermore, it was essential for broadband DCS. The bandwidth is superior to that reported in previous studies on dual-comb fiber lasers [51,52] and other types of dual-comb lasers [43,45]. In subsections 2.4 and 2.6, we describe our evaluation of the coherence of the laser cavity output and generation of an octave-spanning frequency comb by nonlinear spectral broadening with high coherence.

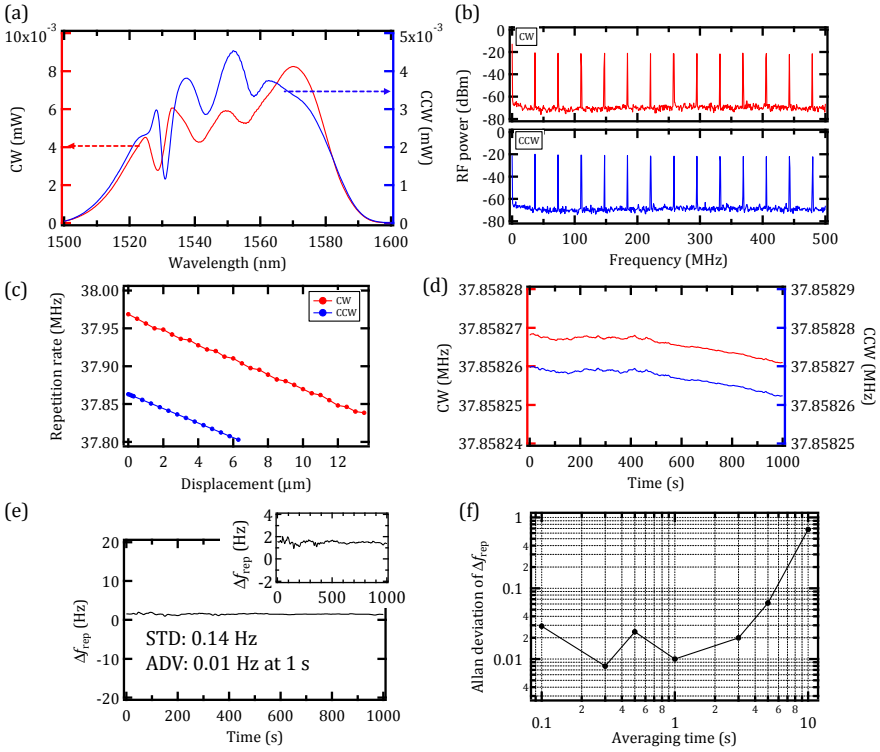

Fig. 2. (a) Optical spectra and (b) RF spectra of the two outputs with a mode-locking operation. (c) Tunability of the repetition rates for the two outputs as a function of the displacement of the collimator in the free-space section. Temporal variation of (d) the repetition rates of the two outputs and (e) the difference in the repetition rate (Δf_{rep}). STD: Standard deviation, ADV: Allan deviation. Inset: Magnified of (e). (f) Allan deviation of Δf_{rep}.

2.3 Stability of dual-comb fiber laser in terms of repetition rate

The radio-frequency (RF) spectra of the two outputs of the developed dual-comb fiber laser are shown in Fig. 2(b). The f_{rep} of the two outputs were approximately 37.9 MHz, with a small difference of $\Delta f_{rep} \approx 1.5$ Hz. As shown in Fig. 2(c), both the f_{rep} values could be varied independently by the position of each collimator in the free-space section. Therefore, Δf_{rep} could be conveniently tuned from a few Hz to a few hundred kHz with positive and negative values. In the CW case, the f_{rep} tuning range was limited by the maximum displacement of the mechanical stage. Meanwhile, in the CCW case, the current mode-locking operation could be maintained through the displacement range of 6.4 μm; this range could be extended by improving the alignment. In DCS, a small Δf_{rep} is essential for achieving a broad spectral bandwidth, which can be measured simultaneously. With $\Delta f_{rep} \approx 1.5$ Hz (f_{rep} = 37.9 MHz), the measurable optical spectral bandwidth ($\Delta\nu = f_{rep}^2 / 2\Delta f_{rep}$) could attain 479 THz ($\Delta\lambda \approx 3{,}888$ nm). We measured the f_{rep}s of the two combs simultaneously using two frequency counters (Tektronics, FCA3100) that refer to an Rb frequency standard (SRS, FS725). Figures 2(d)-2(e) show the temporal variation of f_{rep} of the two outputs and Δf_{rep} in the free-running operation.

Optics EXPRESS

Whereas each f_{rep} fluctuated owing to environmental perturbation, a high relative stability of Δf_{rep} was achieved (a standard deviation of 0.14 Hz; Allan deviation of 0.01 Hz for an averaging time of 1 s) without temperature control; this was owing to passive common-mode noise cancellation. Figure 2(f) shows the Allan deviation of Δf_{rep}; it was stable for the averaging time. This is a significant advantage for DCS, where Δf_{rep} should be maintained constant during multi-heterodyne beat signal measurement. The mode-locking operation could be maintained for a few days without realignment or maintenance. f_{rep} could be further increased by reducing the physical dimensions of the cavity and replacing the two 3-dB couplers and three-port circulators with a simple four-port circulator. Moreover, Δf_{rep} could be further stabilized by stabilizing the laser cavity, e.g., by temperature control.

2.4 Evaluation of coherence for dual-comb fiber laser in both directions

To evaluate the coherence, we detected the beat notes between each frequency comb and a narrow-linewidth single-frequency external-cavity diode laser (ECDL, Toptica DL-pro, linewidth ~10 kHz) at 1,530, 1,550, and 1,580 nm. Figures 3(a)–3(f) show the RF spectra of the beat notes for the two frequency combs in each wavelength region. In all the wavelength regions, we successfully obtained beat notes with a high SNR of ~35 dB at a resolution bandwidth of 100 kHz and narrow linewidth of ~10 kHz, as shown in Figs. 3(g) and 3(h). Furthermore, there were no spikes originating from large phase noise in both directions. These results imply that the two frequency combs with broad spectra exhibited sufficient coherence at approximately 1,550 nm. Such a low phase noise frequency comb from the laser cavity is necessary to generate a high-coherence supercontinuum.

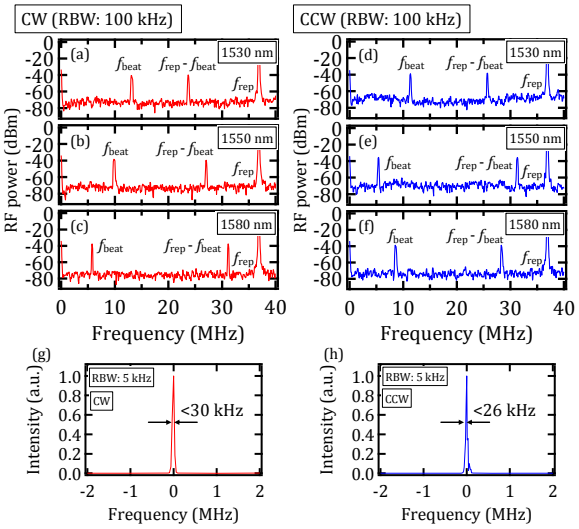

Fig. 3. Beat notes between a single frequency laser and the two outputs in the clockwise (a–c) and counter-clockwise (d-f) directions for 1530–1580 nm with an RBW of 100 kHz. (g–h) Magnified beat plots of (b) and (e) with an RBW of 5 kHz.

2.5 Evaluation of relative coherence between the two outputs

For evaluating the relative coherence between the dual outputs of the laser, we detected the relative beat notes between each frequency comb and a single-frequency ECDL (Toptica, DL-pro) at 1,530, 1,550, and 1,580 nm, which was used as an intermediate laser. The two beat notes for both the frequency combs were extracted by a low-pass filter and amplified by a low-noise RF amplifier. Then, the two beat notes were mixed with a double balanced mixer, and only the difference-frequency signal was extracted by filtering. As shown in Fig. 4(a), the difference-frequency beat note had a linewidth of <1 kHz (for a measurement-duration of 1.9 ms). Here, the measured linewidth was limited

Optics EXPRESS

by the measurement resolution because long time averaging could not be applied without phase locking between the intermediate laser and the comb mode.

In addition, we directly detected the multi-heterodyne beat notes between the two frequency combs with Δf_{rep} ≈30 Hz. The two frequency combs were combined using a 50/50 coupler and launched into a rapid photodetector (Newfocus, 1811) via an optical band-pass filter (BPF) with a bandwidth of ~1 nm at 1,550 nm. Figure 4(b) shows the RF spectra of the detected multi-heterodyne beat note in the case of Δf_{rep} ≈30 Hz. To verify that the beat notes are the multi-heterodyne beat notes between the optical frequency modes of the two combs rather than the mixing products in the RF domain, we changed the center wavelength of the BPF manually; it was observed that the center frequency for the beat note changed. As shown in Fig. 4(c), we obtained mode-resolved multi-heterodyne beat notes with an RF spectrum analyzer (Rohde & Schwarz, FSV-13). These results imply that the two frequency combs from the single-laser cavity exhibited high relative coherence. A comparison of Figs. 4(b) and 4(c) shows that the amplitude of the beat signal varied slightly depending on the measurement resolution, i.e., measurement time. This could be owing to the fluctuation from fiber noise in the beat detection system [50,59] and residual non-common-mode noise in the non-common path in the laser cavity. Applying fiber noise cancellation for beat detection and employing a hermetically sealed box for the non-common path in the laser cavity could have further passively stabilized the beat. Nevertheless, we obtained mode-resolved beat notes with Δf_{rep} ≈30 Hz with a resolution bandwidth (RBW) of 5 Hz. The FWHM of each beat note was 3.8 Hz (Gaussian), and it is limited by an RBW of 5 Hz. Thus, the relative linewidth between the two frequency combs could be 5 Hz or less. This result implies that the developed DCS laser can maintain coherence for over 0.26 s without servo control. With this narrow linewidth, a small Δf_{rep} could be achieved. Thus, broadband DCS can be realized using the developed dual-comb fiber laser.

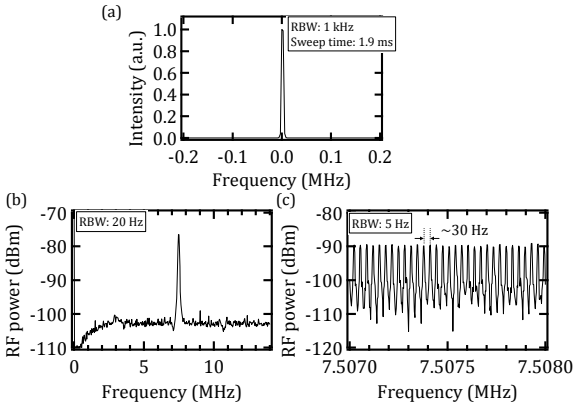

Fig. 4. RF spectra. (a) Relative beat note between a pair of comb teeth from the two frequency combs at 1,550 nm. The beat note has a linewidth of < 1 kHz for a measurement-duration of 1.9 ms. (b) Multi-heterodyne beat notes between the two frequency combs with Δf_{rep} ≈30 Hz. (c) Magnified multi-heterodyne beat notes of (b).

2.6 Generation of ultra-broadband optical frequency comb and detection of carrier–envelope offset frequency beat notes with dual-comb fiber laser

Next, we evaluate the f_{CEO} of the developed dual-comb fiber laser, which is one of the most important parameters of the comb. To detect f_{CEO} beat signals, we generated an ultra-broadband optical frequency comb spanning more than one octave with EDF amplifiers and HNLFs based on the two outputs. The fiber amplifier and HNLF were optimized to generate an octave-spanning frequency comb using dispersion management [60]. For measuring such an octave-spanning spectrum, we used two types of optical spectrum analyzers to cover the entire spectral region (Yokogawa, AQ6370D and AQ6375). As shown in Fig. 5(a), we obtained an ultra-broadband optical frequency comb spanning more than one octave for both the frequency combs.

Optics EXPRESS

For evaluating the coherence of the octave-spanning frequency comb at the far end of the short and long wavelength regions, we detected the RF spectra of the two outputs. Figure 5(b) shows the RF spectra of the two outputs at 1,020 nm and second harmonic generation for 2,040 nm. They are similar to the original RF spectra of the direct outputs from the oscillator, as shown in Fig. 2(b). Moreover, we detected f_{CEO} beat signals using a common-path f–$2f$ interferometer based on a self-referencing scheme [47]. The entire supercontinuum was launched into a periodically poled lithium niobate (PPLN) crystal, and the comb teeth around 2,040 nm were doubled and mixed with the comb teeth around 1,020 nm. From the two ultra-broadband frequency combs for the CW and CCW outputs (Fig. 5(c)), we successfully detected f_{CEO} beat notes simultaneously. The SNR was ~30 dB at a resolution bandwidth of 100 kHz, and the linewidth was ~10 kHz. The results imply that the ultra-broadband frequency combs exhibited sufficient coherence, i.e., low phase noise over one octave even after nonlinear spectral broadening; they also imply that that the obtained SNR could have been measured with a frequency counter. To our knowledge, this is the first demonstration of the direct detection of f_{CEO} beat notes using a self-referencing technique for a dual-comb fiber laser.

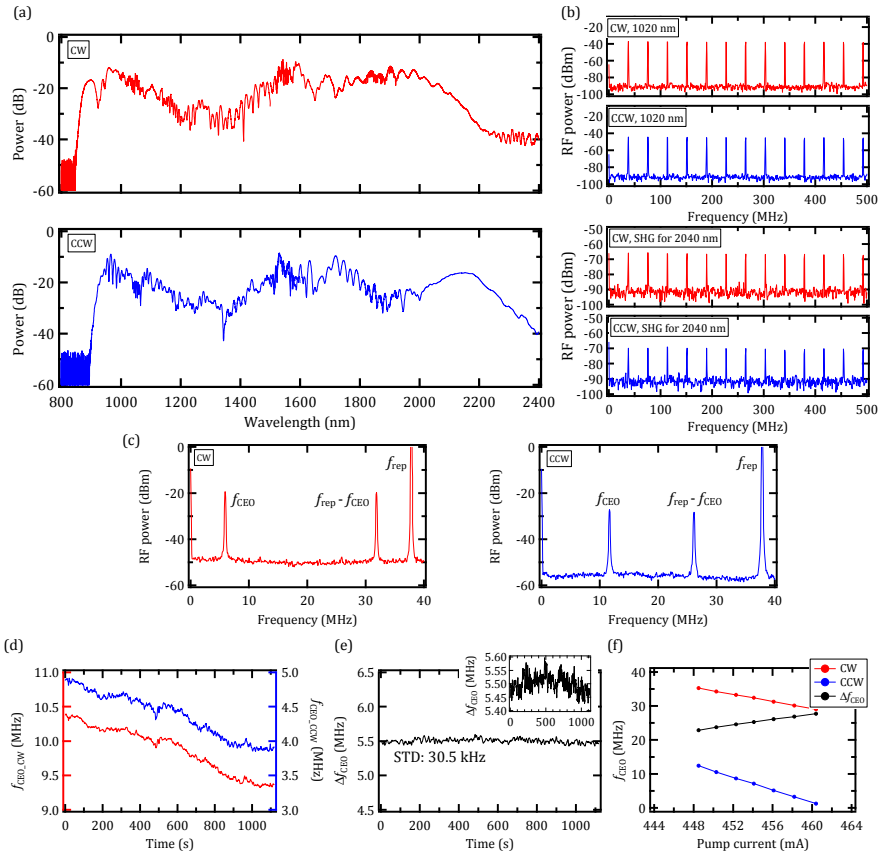

Fig. 5. (a) Optical spectra of broadened optical frequency comb based on bidirectional outputs with Er-doped fiber amplifier (EDFA) and highly nonlinear fiber (HNLF). (b) RF spectra of each output of bidirectional comb at 1,020 nm and second harmonic generation for 2,040 nm. (c) Beat notes of carrier–envelope offset frequency (f_{CEO}) in both directions. Temporal variation of (d) carrier–envelope offset frequencies (f_{CEO}s) of the two outputs and (e) difference in carrier–envelope offset frequency (Δf_{CEO}). Inset: Magnified plots. (f) Tunability of f_{CEO} and Δf_{CEO}.

2.7 Evaluation of carrier–envelope offset frequency of dual-comb fiber laser

For evaluating the two f_{CEO} beat signals, we measured both the signals simultaneously using two frequency counters (Tektronics, FCA3100) that refer to an Rb frequency

Optics EXPRESS

standard (SRS, FS725). Figures 5(d) and 5(e) show the temporal variation in f_{CEO} in both the directions and Δf_{CEO} in the free-running operation. Whereas each f_{CEO} varies by ~1 MHz over 1,000 s owing to environmental perturbation, Δf_{CEO} remained highly stable at ~5.5 MHz with a standard deviation of 30.5 kHz; this was owing to passive common-mode noise cancellation. This is a significant advantage for DCS, where Δf_{CEO} should be maintained constant during the measurement of the multi-heterodyne beat signal. To our knowledge, this is the first demonstration of the direct measurement of f_{CEO} beat notes using a self-referencing scheme for a dual-comb fiber laser. Furthermore, as shown in Fig. 5(f), the two f_{CEO} signals and Δf_{CEO} could be varied by a pump current (I), i.e., pump power; this is important for practical application. The two tuning rates ($\Delta f/\Delta I$) were - 0.53 and - 0.93 MHz/mA, respectively.

To investigate the two f_{CEO} signals in a short-term time scale, we also measured the phase noise of both the f_{CEO} beat signals in free-running operation using a digital phase meter implemented on a field-programmable gate array (FPGA) [61]. Figure 6(a) shows the phase noise of f_{CEO} when the laser operated with unidirectional mode locking. In this case, we changed the operational state by inserting a block in the free-space of the SAMs. A comparison of Figs. 6(a) and 6(b) shows that in the bidirectional mode-locking operation case reveals specific modulation peaks in the range of 1–10 Hz; these were common for both the CW and CCW combs. In contrast, similar peaks were not observed in the unidirectional mode-locking case. This result implies that interaction occurred between the two counter propagating pulses in the frequency combs. As explained in subsection 2.3, in the developed dual-comb fiber laser, the strong nonlinear interaction at the saturable absorber can be avoided using the two-SAM configuration; otherwise, Δf_{rep} cannot attain the order of Hz owing to the self-synchronization between the two frequency combs at the saturable absorber. Meanwhile, the gain fiber is shared between the two frequency combs; thus, interaction via gain can occur. However, such interaction does not seem to degrade the performance since, in the preliminary experiment, common-mode noise reduction in the Δf_{CEO} beat was observed in the RF spectra. In the future, further detailed evaluation of Δf_{CEO} would be performed by applying the developed laser to the spectroscopy. Moreover, the tunability of the two f_{CEO} signals simultaneously by the pump power, as shown in Fig. 5(f), also implies interaction at the gain fiber in the laser cavity. In this case, such controllability of Δf_{CEO} is essential for further stabilizing Δf_{CEO} and for applications such as coherent averaging.

Optics EXPRESS

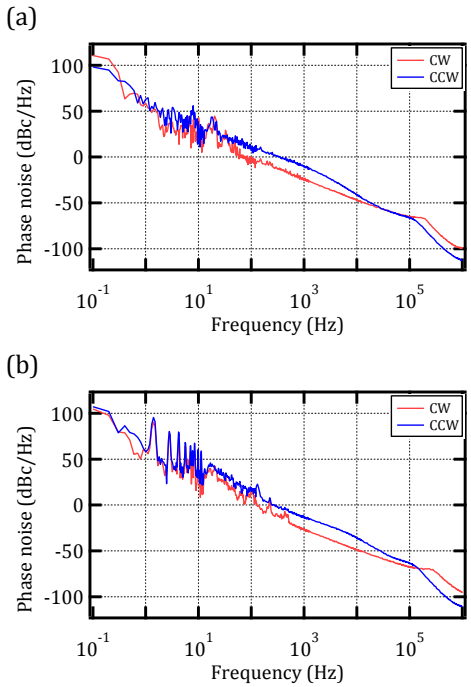

Fig. 6. Phase noise of carrier–envelope offset beat notes in both directions. (a) Unidirectional mode-locking operation. (b) Bidirectional mode-locking operation.

3. Discussion

As described in Section 2.6, we achieved f_{CEO} beat note detection using a self-referencing technique for the developed dual-comb fiber laser; moreover, a high relative stability by common-mode noise cancellation for the two f_{CEO}s was demonstrated. Although the dual-comb fiber laser exhibited the relative stability of Δf_{CEO} in free-running operation, further active stabilization of f_{CEO} and Δf_{CEO} is feasible because of the high SNR of ~30 dB at an RBW of 100 kHz. As demonstrated in Fig. 5(f), the two f_{CEO} beat signals and Δf_{CEO} could be varied by the pump power for the dual-comb fiber laser. Thus, in future, f_{CEO} or Δf_{CEO} can be stabilized by servo control of the pump power. In addition, with stable Δf_{CEO}, coherent averaging, which is an important technique for DCS, can be realized. Similar averaging technique has not been demonstrated for a dual-comb laser. Furthermore, the absolute frequency can be determined using the developed dual-comb fiber laser because the two f_{rep}s and f_{CEO}s can be measured with frequency counters, and Δf_{rep} can be changed by the procedure described in [62]. In contrast, in previous studies [51,52], the absolute frequency was determined using a reference laser or absorption line frequency because the two f_{CEO} beat notes were not detected.

Because the obtained supercontinuum exhibited high coherence over one octave, the two outputs of the developed dual-comb fiber laser can be extended to other wavelength regions by nonlinear optics with high coherence. Visible, mid-infrared, and terahertz generation can be realized via nonlinear frequency conversion. For example, on the basis of the octave-spanning frequency combs between 1,000 and 2,000 nm with high coherence, visible comb generation can be realized using a PPLN waveguide [63]; moreover, mid-infrared comb generation can be realized through difference-frequency generation [64,65]. In addition, for terahertz spectroscopy based on the DCS technique, Δf_{rep} is an important factor owing to the terahertz detection system bandwidth limitation [66]. For our developed dual-comb fiber laser, the tunability of Δf_{rep} by changing the length in the separated region is suitable for terahertz spectroscopy.

Optics EXPRESS

4. Conclusion

We developed a high-coherence ultra-broadband bidirectional dual-comb fiber laser to realize a simple and robust ultra-broadband DCS system for practical applications. We successfully detected the high SNR f_{CEO} beat notes for the two frequency combs in both directions; moreover, a high relative stability between the two f_{CEO} beat signals was demonstrated. To our knowledge, this is the first demonstration of f_{CEO} detection and frequency measurement using a self-referencing technique for a dual-comb fiber laser. In addition, a highly small Δf_{rep} (< 1.5 Hz; f_{rep} = 38 MHz) with high relative stability was demonstrated. Because of this small Δf_{rep}, the applicable optical spectral bandwidth in DCS could attain ~479 THz (~3,888 nm). As these two frequency combs are generated by the same single-laser cavity, the mutual coherence between the two frequency combs is high owing to passive common-mode noise cancellation. The detection and regulation of f_{CEO} is required in various dual-comb spectroscopy applications such as high-precision spectroscopy with absolute frequency accuracy, high-sensitivity detection using coherent averaging, coherent spectroscopy, nonlinear spectroscopy, and phase imaging. Moreover, broad spectral coverage with high coherence could be extended to other wavelength regions such as visible, mid-infrared, and terahertz by nonlinear frequency conversion. Because the fiber-based configuration is robust and compact, the developed dual-comb fiber laser is likely to be a highly effective tool in practical ultra-broadband spectroscopy with high coherence for a broad range of applications. We consider our dual-comb fiber laser to be a potential alternative to the current sophisticated DCS system; furthermore, the proposed system can expand the range of application of optical frequency combs. The laser can be used for DCS as well as for other applications such as asynchronous optical sampling [67] and optical coherence tomography [68].

Funding

Japan Science and Technology Agency (JST); Exploratory Research for Advanced Technology (ERATO) MINOSHIMA Intelligent Optical Synthesizer (IOS) Project (JPMJER1304).

Acknowledgments

We thank Ken'ichi Kondo (UEC) for his assistance in the early stages of the development of the laser. We also thank Zheng Zheng (Beihang Univ.) for the fruitful discussions; Akiko Nishiyama (UEC) and Takeshi Yasui (Tokushima Univ.) for their valuable advice regarding the DCS system; and Masaaki Hirano, Yoshinori Yamamoto, and Takemi Hasegawa of Sumitomo Electronic Industries, Ltd. for providing us with highly nonlinear fibers.

References

1. J. L. Hall, "Nobel lecture: defining and measuring optical frequencies," Rev. Mod. Phys. **78**(4), 1279–1295 (2006).
2. T. W. Hänsch, "Nobel Lecture: Passion for precision," Rev. Mod. Phys. **78**(4), 1297–1309 (2006).
3. R. Holzwarth, T. Udem, T. W. Hänsch, J. C. Knight, W. J. Wadsworth, and P. St. J. Russell, "Optical frequency synthesizer for precision spectroscopy," Phys. Rev. Lett. **85**(11), 2264–2267 (2000).
4. D. J. Jones, S. A. Diddams, J. K. Ranka, A. Stentz, R. S. Windeler, J. L. Hall, and S. T. Cundiff, "Carrier-envelope phase control of femtosecond mode-locked lasers and direct optical frequency synthesis," Science **288**(5466), 635–640 (2000).
5. H. Telle, G. Steinmeyer, A. Dunlop, J. Stenger, D. Sutter, and U. Keller, "Carrier-envelope offset phase control: A novel concept for absolute optical frequency measurement and ultrashort pulse generation," Appl. Phys. B **69**(4), 327–332 (1999).
6. R. J. Jones, W. Y. Cheng, K. W. Holman, L.-S. Chen, J. L. Hall, and J. Ye, "Absolute-frequency measurement of the iodine-based length standard at 514.67 nm," Appl. Phys. B **74**(6), 597–601 (2002).
7. S. A. Diddams, T. Udem, J. C. Bergquist, E. A. Curtis, R. E. Drullinger, L. Hollberg, W. M. Itano, W. D. Lee, C. W. Oates, K. R. Vogel, and D. J. Wineland, "An optical clock based on a single trapped 199Hg+ ion," Science **293**(5531), 825–828 (2001).
8. M. Takamoto, F.-L. Hong, R. Higashi, and H. Katori, "An optical lattice clock," Nature **435**(7040), 321–324 (2005).
9. Th. Udem, J. Reichert, R. Holzwarth, and T. W. Hänsch, "Absolute optical frequency measurement of the Cesium D1 line with a mode-locked laser," Phys. Rev. Lett. **82**(18), 3568–3571 (1999).

Optics EXPRESS

10. S. A. Diddams, L. Hollberg, and V. Mbele, "Molecular fingerprinting with the resolved modes of a femtosecond laser frequency comb," Nature **445**(7128), 627–630 (2007).
11. T. M. Fortier, M. S. Kirchner, F. Quinlan, J. Taylor, J. C. Bergquist, T. Rosenband, N. Lemke, A. Ludlow, Y. Jiang, C. W. Oates, and S. A. Diddams, "Generation of ultrastable microwaves via optical frequency division," Nat. Photonics **5**(7), 425–429 (2011).
12. X. Xie, R. Bouchand, D. Nicolodi, M. Giunta, W. Hänsel, M. Lezius, A. Joshi, S. Datta, C. Alexandre, M. Lours, P.-A. Tremblin, G. Santarelli, R. Holzwarth, and Y. Le Coq, "Photonic microwave signals with zeptosecond-level absolute timing noise," Nat. Photonics **11**(1), 44–47 (2017).
13. D. Hillerkuss, R. Schmogrow, T. Schellinger, M. Jordan, M. Winter, G. Huber, T. Vallaitis, R. Bonk, P. Kleinow, F. Frey, M. Roeger, S. Koenig, A. Ludwig, A. Marculescu, J. Li, M. Hoh, M. Dreschmann, J. Meyer, S. Ben Ezra, N. Narkiss, B. Nebendahl, F. Parmigiani, P. Petropoulos, B. Resan, A. Oehler, K. Weingarten, T. Ellermeyer, J. Lutz, M. Moeller, M. Huebner, J. Becker, C. Koos, W. Freude, and J. Leuthold, "26 Tbit s−1 line-rate super-channel transmission utilizing all-optical fast Fourier transform processing," Nat. Photonics **5**(6), 364–371 (2011).
14. S. T. Cundiff and A. M. Weiner, "Optical arbitrary waveform generation," Nat. Photonics **4**(11), 760–766 (2010).
15. T. Wilken, G. L. Curto, R. A. Probst, T. Steinmetz, A. Manescau, L. Pasquini, J. I. González Hernández, R. Rebolo, T. W. Hänsch, T. Udem, and R. Holzwarth, "A spectrograph for exoplanet observations calibrated at the centimetre-per-second level," Nature **485**(7400), 611–614 (2012).
16. R. A. McCracken, J. M. Charsley, and D. T. Reid, "A decade of astrocombs: recent advances in frequency combs for astronomy," Opt. Express **25**(13), 15058–15078 (2017).
17. K. Minoshima and H. Matsumoto, "High-accuracy measurement of 240-m distance in an optical tunnel by use of a compact femtosecond laser," Appl. Opt. **39**(30), 5512–5517 (2000).
18. C. Gohle, B. Stein, A. Schliesser, T. Udem, and T. W. Hänsch, "Frequency comb Vernier spectroscopy for broadband, high-resolution, high-sensitivity absorption and dispersion spectra," Phys. Rev. Lett. **99**(26), 263902 (2007).
19. M. J. Thorpe and J. Ye, "Cavity-enhanced direct frequency comb spectroscopy," Appl. Phys. B **91**(3-4), 397–414 (2008).
20. J. Mandon, G. Guelachvili, and N. Picqué, "Fourier transform spectroscopy with a laser frequency comb," Nat. Photonics **3**(2), 99–102 (2009).
21. A. Foltynowicz, T. Ban, P. Masłowski, F. Adler, and J. Ye, "Quantum-noise-limited optical frequency comb spectroscopy," Phys. Rev. Lett. **107**(23), 233002 (2011).
22. F. Keilmann, C. Gohle, and R. Holzwarth, "Time-domain mid-infrared frequency-comb spectrometer," Opt. Lett. **29**(13), 1542–1544 (2004).
23. I. Coddington, W. C. Swann, and N. R. Newbury, "Coherent multiheterodyne spectroscopy using stabilized optical frequency combs," Phys. Rev. Lett. **100**(1), 013902 (2008).
24. S. Okubo, Y.-D. Hsieh, H. Inaba, A. Onae, M. Hashimoto, and T. Yasui, "Near-infrared broadband dual-frequency-comb spectroscopy with a resolution beyond the Fourier limit determined by the observation time window," Opt. Express **23**(26), 33184–33193 (2015).
25. I. Coddington, N. R. Newbury, and W. C. Swann, "Dual-comb spectroscopy," Optica **3**(4), 414–426 (2016).
26. S. Okubo, K. Iwakuni, H. Inaba, K. Hosaka, A. Onae, H. Sasada, and F.-L. Hong, "Ultra-broadband dual-comb spectroscopy across 1.0-1.9 μm," Appl. Phys. Express **8**(8), 082402 (2015).
27. A. Nishiyama, S. Yoshida, Y. Nakajima, H. Sasada, K. Nakagawa, A. Onae, and K. Minoshima, "Doppler-free dual-comb spectroscopy of Rb using optical-optical double resonance technique," Opt. Express **24**(22), 25894–25904 (2016).
28. T. Minamikawa, Y. D. Hsieh, K. Shibuya, E. Hase, Y. Kaneoka, S. Okubo, H. Inaba, Y. Mizutani, H. Yamamoto, T. Iwata, and T. Yasui, "Dual-comb spectroscopic ellipsometry," Nat. Commun. **8**(1), 610 (2017).
29. A. Asahara, A. Nishiyama, S. Yoshida, K. I. Kondo, Y. Nakajima, and K. Minoshima, "Dual-comb spectroscopy for rapid characterization of complex optical properties of solids," Opt. Lett. **41**(21), 4971–4974 (2016).
30. A. Asahara and K. Minoshima, "Development of ultrafast time-resolved dual-comb spectroscopy," APL Photonics **2**(4), 041301 (2017).
31. T. Ideguchi, S. Holzner, B. Bernhardt, G. Guelachvili, N. Picqué, and T. W. Hänsch, "Coherent Raman spectro-imaging with laser frequency combs," Nature **502**(7471), 355–358 (2013).
32. A. Nishiyama, Y. Nakajima, K. Nakagawa, and K. Minoshima, "Precise and highly-sensitive Doppler-free two-photon absorption dual-comb spectroscopy using pulse shaping and coherent averaging for fluorescence signal detection," Opt. Express **26**(7), 8957–8967 (2018).
33. Y.-D. Hsieh, Y. Iyonaga, Y. Sakaguchi, S. Yokoyama, H. Inaba, K. Minoshima, F. Hindle, T. Araki, and T. Yasui, "Spectrally interleaved, comb-mode-resolved spectroscopy using swept dual terahertz combs," Sci. Rep. **4**(1), 3816 (2014).
34. N. Kuse, A. Ozawa, and Y. Kobayashi, "Static FBG strain sensor with high resolution and large dynamic range by dual-comb spectroscopy," Opt. Express **21**(9), 11141–11149 (2013).
35. S. Coburn, C. B. Alden, R. Wright, K. Cossel, E. Baumann, C.-W. Truong, F. Giorgetta, C. Sweeney, N. R. Newbury, K. Prasad, I. Coddington, and G. R. Rieker, "Regional trace-gas source attribution using a field-deployed dual frequency comb spectrometer," Optica **5**(4), 320–327 (2018).
36. T.-A. Liu, N. R. Newbury, and I. Coddington, "Sub-micron absolute distance measurements in sub-millisecond times with dual free-running femtosecond Er fiber-lasers," Opt. Express **19**(19), 18501–18509 (2011).

Optics EXPRESS

37. E. Hase, T. Minamikawa, T. Mizuno, S. Miyamoto, R. Ichikawa, Y.-D. Hsieh, K. Shibuya, K. Sato, Y. Nakajima, A. Asahara, K. Minoshima, Y. Mizutani, T. Iwata, H. Yamamoto, and T. Yasui, "Scan-less confocal phase imaging based on dual-comb microscopy," Optica **5**(5), 634–643 (2018).
38. K. Shibuya, T. Minamikawa, Y. Mizutani, H. Yamamoto, K. Minoshima, T. Yasui, and T. Iwata, "Scan-less hyperspectral dual-comb single-pixel-imaging in both amplitude and phase," Opt. Express **25**(18), 21947–21957 (2017).
39. J. Roy, J.-D. Deschênes, S. Potvin, and J. Genest, "Continuous real-time correction and averaging for frequency comb interferometry," Opt. Express **20**(20), 21932–21939 (2012).
40. T. Ideguchi, A. Poisson, G. Guelachvili, N. Picqué, and T. W. Hänsch, "Adaptive real-time dual-comb spectroscopy," Nat. Commun. **5**(1), 3375 (2014).
41. G.-W. Truong, E. M. Waxman, K. C. Cossel, E. Baumann, A. Klose, F. R. Giorgetta, W. C. Swann, N. R. Newbury, and I. Coddington, "Accurate frequency referencing for fieldable dual-comb spectroscopy," Opt. Express **24**(26), 30495–30504 (2016).
42. L. C. Sinclair, I. Coddington, W. C. Swann, G. B. Rieker, A. Hati, K. Iwakuni, and N. R. Newbury, "Operation of an optically coherent frequency comb outside the metrology lab," Opt. Express **22**(6), 6996–7006 (2014).
43. N. B. Hébert, J. Genest, J.-D. Deschênes, H. Bergeron, G. Y. Chen, C. Khurmi, and D. G. Lancaster, "Self-corrected chip-based dual-comb spectrometer," Opt. Express **25**(7), 8168–8179 (2017).
44. T. Ideguchi, T. Nakamura, Y. Kobayashi, and K. Goda, "Kerr-lens mode-locked bidirectional dual-comb ring laser for broadband dual-comb spectroscopy," Optica **3**(7), 748–753 (2016).
45. S. M. Link, D. J. H. C. Maas, D. Waldburger, and U. Keller, "Dual-comb spectroscopy of water vapor with a free-running semiconductor disk laser," Science **356**(6343), 1164–1168 (2017).
46. A. Dutt, C. Joshi, X. Ji, J. Cardenas, Y. Okawachi, K. Luke, A. L. Gaeta, and M. Lipson, "On-chip dual-comb source for spectroscopy," Sci. Adv. **4**(3), e1701858 (2018).
47. T. R. Schibli, K. Minoshima, F.-L. Hong, H. Inaba, A. Onae, H. Matsumoto, I. Hartl, and M. E. Fermann, "Frequency metrology with a turnkey all-fiber system," Opt. Lett. **29**(21), 2467–2469 (2004).
48. B. R. Washburn, S. A. Diddams, N. R. Newbury, J. W. Nicholson, M. F. Yan, and C. G. Jørgensen, "Phase-locked, erbium-fiber-laser-based frequency comb in the near infrared," Opt. Lett. **29**(3), 250–252 (2004).
49. H. Inaba, Y. Daimon, F.-L. Hong, A. Onae, K. Minoshima, T. R. Schibli, H. Matsumoto, M. Hirano, T. Okuno, M. Onishi, and M. Nakazawa, "Long-term measurement of optical frequencies using a simple, robust and low-noise fiber based frequency comb," Opt. Express **14**(12), 5223–5231 (2006).
50. Y. Nakajima, H. Inaba, K. Hosaka, K. Minoshima, A. Onae, M. Yasuda, T. Kohno, S. Kawato, T. Kobayashi, T. Katsuyama, and F.-L. Hong, "A multi-branch, fiber-based frequency comb with millihertz-level relative linewidths using an intra-cavity electro-optic modulator," Opt. Express **18**(2), 1667–1676 (2010).
51. X. Zhao, G. Hu, B. Zhao, C. Li, Y. Pan, Y. Liu, T. Yasui, and Z. Zheng, "Picometer-resolution dual-comb spectroscopy with a free-running fiber laser," Opt. Express **24**(19), 21833–21845 (2016).
52. S. Mehravar, R. A. Norwood, N. Peyghambarian, and K. Kieu, "Real-time dual-comb spectroscopy with a free-running bidirectionally mode-locked fiber laser," Appl. Phys. Lett. **108**(23), 231104 (2016).
53. Y. H. Ou, J. Olson, S. Mehravar, R. A. Norwood, N. Peyghambarian, and K. Kier, "Octave-spanning dual-comb spectroscopy with a free-running bidirectional mode-locked femtosecond fiber laser," in CLEO (OSA, San Jose, CA, 2017), SM2L.3.
54. G. Hu, Y. Pan, X. Zhao, S. Yin, M. Zhang, and Z. Zheng, "Asynchronous and synchronous dual-wavelength pulse generation in a passively mode-locked fiber laser with a mode-locker," Opt. Lett. **42**(23), 4942–4945 (2017).
55. C. Ouyang, P. Shum, K. Wu, J.-H. Wong, H.-Q. Lam, and S. Aditya, "Bidirectional passively mode-locked soliton fiber laser with a four-port circulator," Opt. Lett. **36**(11), 2089–2091 (2011).
56. F. X. Kurtner, J. A. der Au, and U. Keller, "Mode-locking with slow and fast saturable absorbers—what's the difference?" IEEE J. Sel. Top. Quantum Electron. **4**(2), 159–168 (1998).
57. S. Kim, Y. Kim, J. Park, S. Han, S. Park, Y.-J. Kim, and S.-W. Kim, "Hybrid mode-locked Er-doped fiber femtosecond oscillator with 156 mW output power," Opt. Express **20**(14), 15054–15060 (2012).
58. F.-L. Hong, K. Minoshima, A. Onae, H. Inaba, H. Takada, A. Hirai, H. Matsumoto, T. Sugiura, and M. Yoshida, "Broad-spectrum frequency comb generation and carrier-envelope offset frequency measurement by second-harmonic generation of a mode-locked fiber laser," Opt. Lett. **28**(17), 1516–1518 (2003).
59. K. Kashiwagi, Y. Nakajima, M. Wada, S. Okubo, and H. Inaba, "Multi-branch fiber comb with relative frequency uncertainty at 10^{-20} using fiber noise difference cancellation," Opt. Express **26**(7), 8831–8840 (2018).
60. Y. Nakajima, H. Inaba, F.-L. Hong, A. Onae, K. Minoshima, T. Kobayashi, M. Nakazawa, and H. Matsumoto, "Optimized amplification of femtosecond optical pulses by dispersion management for octave-spanning optical frequency comb generation," Opt. Commun. **281**(17), 4484–4487 (2008).
61. W. Kokuyama, H. Nozato, A. Ohta, and K. Hattori, "Simple digital phase-measurement algorithm for low-noise heterodyne interferometry," Meas. Sci. Technol. **27**(8), 085001 (2016).
62. H. Inaba, Y. Nakajima, F.-L. Hong, K. Minoshima, J. Ishikawa, A. Onae, H. Matsumoto, M. Wouters, B. Warrington, and N. Brown, "Frequency measurement capability of a fiber-based frequency comb at 633 nm," IEEE Trans. Instrum. Meas. **58**(4), 1234–1240 (2009).
63. K. Iwakuni, S. Okubo, O. Tadanaga, H. Inaba, A. Onae, F.-L. Hong, and H. Sasada, "Generation of a frequency comb spanning more than 3.6 octaves from ultraviolet to mid infrared," Opt. Lett. **41**(17), 3980–3983 (2016).
64. G. Ycas, F. R. Giorgetta, E. Baumann, I. Coddington, D. Herman, S. A. Diddams, and N. R. Newbury, "High-coherent mid-infrared dual-comb spectroscopy spanning 2.6 to 5.2 μm," Nat. Photonics **12**(4), 202–208 (2018).

Optics EXPRESS

65. H. Timmers, A. Kowligy, A. Lind, F. C. Cruz, N. Nader, M. Silfies, G. Ycas, T. K. Allison, P. G. Schunemann, S. B. Papp, and S. A. Diddams, "Molecular fingerprinting with bright, broadband infrared frequency combs," Optica **5**(6), 727–732 (2018).
66. G. Hu, T. Mizuguchi, R. Oe, K. Nitta, X. Zhao, T. Minamikawa, T. Li, Z. Zheng, and T. Yasui, "Dual terahertz comb spectroscopy with a single free-running fibre laser," Sci. Rep. **8**(1), 11155 (2018).
67. A. Bartels, R. Cerna, C. Kistner, A. Thoma, F. Hudert, C. Janke, and T. Dekorsy, "Ultrafast time-domain spectroscopy based on high-speed asynchronous optical sampling," Rev. Sci. Instrum. **78**(3), 035107 (2007).
68. S.-J. Lee, B. Widiyatmoko, M. Kourogi, and M. Ohtsu, "Ultrahigh scanning speed optical coherence tomography using optical frequency comb generator," Jpn. J. Appl. Phys. **40**(Part 2, No. 8B), L878–L880 (2001).